"The stages in the stress-strain curve have been shown to correspond with stages in band formation and propagation."

Kinetics of Shear Band Formation and Propagation in Glassy Polycarbonate Deformed in Simple Shear

by

Adolfo Jesus R. Gopez, Dr. –Ing*

Abstract

A technique involving surface marking of simple shear test specimens was used to investigate the formation of shear bands in polycarbonate. Plane simple shear testing was done to produce a single shear band in the test specimen. Testing was done at ambient temperature (T = 23 ± 1 °C) and at a constant reference shear strain rate ($\dot{\gamma} = 3\ 10^{-3}\ s^{-1}$). Results showed that the shear band formed at yield and then propagated in two stages: first by elongation and later by widening. On the shear stress vs. shear strain curve, the elongation stage corresponded to a stress drop after yield and the widening stage corresponded to plastic deformation with a low apparent strain hardening rate. Observation with markers showed that upon retesting, a previously deformed specimen no longer formed a shear band at yield. Instead it deformed uniformly and homogeneously. End effects were also explored. The results of this study confirm previously obtained results in the preliminary testing of polycarbonate. Shear band formation and propagation were related to a defect theory of plastic deformation for glassy amorphous polymers. According to this theory, plastic deformation takes place when there are enough elementary defects or when these defects are made to move at the right velocity. Shear band formation was then explained to be the consequence of the difficulty with which elementary defects could be formed.

Introduction

The plane simple shear test was developed as a means of acquiring supplementary data on the plastic strain behavior of polymeric materials (Boni, 1981; G'sell et al., 1983). Initial application of the test to the case polythylene has given interesting results. The different stress field involved in simple shear has led to the acquisition of data which are complementary to those obtained by other methods. It was particularly observed that simple shear test results are easier to interpret than torsion test results (Gopez, 1983) and that simple shear testing is free from cross-sectional area changes in the specimen (Boni, 1981; Gopez, 1983 and 1984).

The simple shear test was also applied extensively to the case of polycarbonate, an amorphous polymer which is in the glassy state at room temperature

* Professor of Metallurgy, Dept. of Metallurgical and Mining Engineering, U.P. College of Engineering, Diliman, Quezon City.

(Gopez, 1984; G'sell and Gopez, 1984). The shear stress-shear strain curve obtained at room temperature is reproduced in Figure 1. It has been divided into five distinct stages. Results also indicated the formation of a single shear band under the same conditions for which the curve in Figure 1 was obtained. The general features of band formation and growth were shown by a figure in a previous article (Gopez, 1984) which is reproduced in Figure 2. The stages in the stress-strain curve have been shown to correspond with stages in band formation and propagation as follows (Gopez, 1984):

a) Stage I, viscoelastic deformation: all strain is recoverable, no shear band formation.

b) Stage II, stress drop at yield: shear band nucleates; it is narrow and shorter than the test specimen. As the stress drops after yield, the shear band propagates by elongation.

c) Stage III, linear plastic deformation with low apparent strain hardening coefficient: shear band widens during this stage.

d) Stage IV, homogeneous plastic deformation with a high strain hardening coefficient: deformation continues with increasing strain in the shear band. No new shear band forms elsewhere.

The main objective of this study is to explore the shear band phenomenon in more detail and obtain more information on the nature of the plastic deformation mechanism which was proposed previously (G'sell and Jonas, 1981; Gopez, 1984) for glassy amorphous polymers.

Experimental Procedure

Material

The same polycarbonate (Makrolon) used in the initial shear tests was used for this study. The characteristics of the polycarbonate are given elsewhere (Gopez, 1984). Some of the important properties are again cited below:

Number average molecular weight	M_n = 15600 g/mole
Weight average molecular weight	M_w = 28800 g/mole
Polydispersity	1.85
Average degree of polymerization	60 monomers/molecule
Young's Modulus	2200 MPa (DIN 53457)
Birefringence	$5\ 10^{-5}$

The starting material has low initial birefringence which indicates very little molecular orientation. It may be considered to be isotropic.

Test Method

The plane simple shear test as developed by Boni (1981) and G'sell (et al., 1983) is the main mechanical testing method employed in this study. A description of this test is already given elsewhere (G'sell et al., 1983; Gopez, 1984).

Test Specimens

To study the shear band evolution, reference marks were put on a surface of the specimen's calibrated part by fabricating modified test specimens as shown in Figure 3a. The general configuration is similar to that of a conventional speci-

men (Figure 3b) but the specimen is machined such that the grips and the calibrated part are on the same plane. The normal shape of the grips is restored by putting small plates of polycarbonate held in place by the specimen mounting screws. The face to be marked and investigated is polished beforehand. The specimen dimensions remain the same as in a conventional specimen, L = 60 mm, h = 4 mm, e = 3 mm. The reference marks on the polished face of the specimen are made such that they are parallel to each other and perpendicular to the shear stress direction. The marks were made by passing the specimen on fine abrasive paper (1200P grit) by means of a reciprocating movement.

Measurement of Local Shear Strain

Deformation by shear would be indicated by the deviation of the markers. The angle of deviation of these markers in the deformed areas was measured with the aid of a rotating platform mounted on an optical microscope. The tangent of this angle, tan θ gives the value of the local shear strain ($\gamma_{loc} = \tan \theta$).

Interrupted Shear Tests

The shear test of a modified specimen was interrupted at different points in the stress-strain curve to monitor the formation and propagation of the shear band and to measure the plastic strain in the band. The following procedure was adopted:

a) interruption of the shear test by means of the "hold" function of the MTS functions generator;

b) unloading of the applied charge on the specimen by controlled movement of the piston of the testing machine (MTS 810);

c) half-hour wait in the unloaded state to allow for the recovery of non-plastic strains;

d) removal of test specimen from shearing apparatus;

e) observations;

f) remounting of specimen on shear test apparatus;

g) continuation of shearing up to another point of the stress-strain curve at which the above-stated operations are renewed.

For this study all of the tests where done at ambient temperature (23±1°C) and at a constant reference strain rate of $3 \cdot 10^{-3}$ s^{-1}.

Observation Techniques

Observations on a microscopic level were done on modified specimens subjected to the interrupted shear test. An optical microscope (Reichert) was used for this purpose. Where they are needed, photomicrographs were obtained by using an Olympus OM2 camera equipped with a microscope attachment. As previously stated, the angle of deviation of the reference markers was measured with a vernier-equipped rotating platform mounted on the microscope. Shear band dimensions were measured on the resulting photomicrographs.

Results

Shear Band Formation and Propagation

The series of photographs in Figure 4 shows the formation and propagation of the shear band as viewed by means of the markers on a modified specimen. Inter-

rupted shear testing at ambient temperature was used to obtain these photomicrographs. These photographs represent the central area of the same test specimen at different points in the stress-strain curve.

Shear strains measured in this study are defined as follows:

a) Local plastic shear strain γ_{Bpl} is the plastic strain in the shear band measured after removal of the applied external stress. It is equal to tan θ where θ is the angle of deviation of the reference markers.

b) Average plastic shear strain γ_{pl} is the plastic strain in the whole calibrated part of the test specimen. $\gamma_{pl} = x/h$ where x is the relative displacement of the specimen grips measured with a caliper, and h = 4mm, the width of the specimen's calibrated part. The smallest division measured by the caliper used in this study was 2/100 mm.

c) Theoretical or calculated average plastic shear strain, $\gamma_{pl,\,calc}$ is obtained by assuming that all of the plastic strain of the specimen is concentrated in the shear band. It is given by the expression:

$$\gamma_{pl,\,calc} = \gamma_{Bpl}\,(h_B/h)\,(L_B/L)$$

where h and L are respectively the width and length of the specimen's calibrated part; and h_B and L_B are respectively the width and length of the shear band.

The results will now be given in reference to the stages of deformation of the shear stress-shear strain curve (see also Gopez, 1984 for supplementary details).

Stage I Viscoelastic Deformation: Deformation during this stage is not permanent. Figure 4a shows that the markers on the specimen remain straight after removal of the externally applied stress.

Stage II Stress Maximum and Stress Drop at Yield: The shear band forms at the beginning of stage II. At this point the band is narrow (h_B = 0.1 mm) and shorter than the specimen (L_B is from 25 to 33 mm). Figure 4b, taken just after yield shows that the local plastic shear strain is similar to the type of deformation which is obtained on a macroscopic level (see Figure 2). The angle of deviation of the markers varies from 24° to 34° (in different specimens) and the local plastic shear strain γ_{Bpl} (= tan θ) must range from 0.5 to 0.7 at the moment the band is formed. These values compare favorably with the strain $\gamma = 0.7$ reported by Wu and Turner (1973) in newly formed shear bands in polycarbonate deformed in torsion.

Figure 5a shows the tip of a newly formed shear band. Going along the band towards the tip, there is a gradual change from a region of deformed material to a region of undeformed material (no band). This is more explicitly shown by Figure 5b. The curve indicates the variation of the local plastic shear strain γ_{Bpl} along the shear band length. The transition region at the band tip extends over an area of length ℓ = 4mm. This will be referred to as the shear band front. It can be divided into a central region of length z = 2.5mm in which the shear strain increases linearly ($d\gamma_{Bpl}/dx = 0.2mm^{-1}$, constant) and two end zones in which the slope of the curve varies rapidly towards a zero value.

A comparison of Figures 4b and 5a shows that the shear band width is not constant along its length. The band is slightly narrower at its ends than at the middle. The band parameter h_B used in this study will be the average band width.

To determine the distribution of plastic strain in the specimen, the average plastic shear strain γ_{pl} (=x/h) was compared with the calculated average plastic shear strain, $\gamma_{pl,\ calc}$. For the specimen used in Figure 4, at the beginning of Stage II (Figure 4b) the plastic shear strain in the band, γ_{Bpl} is 0.67. Since this particular band is 32mm long (L_B) and 0.13mm wide (h_B), $\gamma_{pl,\ calc} = 0.01$ while $\gamma_{pl} = 0.02$. These two values can be considered to be in agreement since the measurement of small strain values has possible errors of the same order of magnitude as the strain values just cited.

During the stress drop following yield the shear band becomes longer until at the end of Stage II the band is as long as the specimen (see Figure 2c).

Stage III Shear Band Widening: The plastic shear strain in the band γ_{Bpl} increases slightly even as the band itself widens during this stage. For the specimen in Figure 4c, $h_B = 0.75$ mm and $\gamma_{Bpl} = 0.78$ while for Figure 4d (taken in Stage III); $h_B = 2.4$ mm and $\gamma_{Bpl} = 0.87$. Figure 6 shows the comparison between γ_{Bpl} and γ_{pl} and $\gamma_{pl,\ calc}$, and γ_{pl}. The curve in Figure 6 shows that the shear band does indeed accommodate all the plastic strain while the material beside the shear band must be essentially undeformed.

At the end of Stage III the shear band occupies the whole calibrated part of the test specimen. At this point plastic shear strain in the band ($\gamma_{Bpl} = \gamma_{pl}$) ranges from 0.80 to 0.90. Plastic deformation in the succeeding stages must take place in the whole specimen rather than in an isolated portion of the specimen.

Stage IV Homogeneous Deformation Stage: Study of markers indicates uniform deviation (and hence homogeneous plastic strain) along the width of the specimen's calibrated part. A gradual increase of γ_{Bpl} (= γ_{pl}) takes place. Figure 4e shows the central portion of the band at this stage. No new shear bands are observed to form at this stage. The maximum observed local plastic strain, γ_{Bpl} is equal to 1.2.

The evolution of the shear band parameters (as shown in Figure 7) during a shear test is shown by Figure 8. This curves were obtained by measuring the parameters in several test specimens.

Specimens Subjected to a Plastic Deformation Cycle: "Cycled Specimens"

Figure 9 shows a series of photomicrographs taken of the same area in a specimen which underwent an initial plastic deformation cycle (called "cycled specimen" in this study) and which was then retested in reverse shear. Figure 9a shows the specimen deformed up to the end of Stage III. Most of the specimen's calibrated part has undergone shear as shown by the deviation of the markers. The shear band is in the area where the markers have been deviated. The specimen is then brought back to zero shear strain and Figure 9b shows that at this point the markers are almost straight. Outlines of the band can still be seen, however. Macroscopically the specimen resembles an undeformed one. Figure 9c shows that upon reshearing plastic deformation takes place homogeneously without formation of another shear band. These results confirm those given in a previous paper (Gopez, 1984).

Shear stress vs. shear strain curves obtained with cycled specimens vary from those obtained with previously undeformed or annealed specimens. Figure 19 shows a curve obtained with a cycled specimen. In this case reshearing was done in the same direction as the original shear direction. For a reverse shear curve refer to a previous article (Gopez, 1984).

Stress-strain curves obtained from cycled specimens are thought to give the intrinsic mechanical response curve of the tested material (Gopez, 1983 and 1984; G'sell and Gopez, 1984). Reference to these response curves will be made later in the discussion of test results.

End Effects

The evolution of the band at a specimen end is given in Figure 10. These photomicrographs show that the shear band tends to pinch off and curve into the specimen grips. These observations confirm that the stress field at the specimen ends deviates from simple shear. Similar findings regarding sheared polycarbonate are cited elsewhere (Gopez, 1984).

It can also be verified from the photomicrographs in Figure 10 that the perturbation at the specimen ends is spread over an area whose dimension is approximately the same as the width of the specimen's calibrated part. Considering that this width is 4 mm and that the specimen length is 60 mm, then it may be safely said that simple shear conditions prevail in most of the specimen. This conclusion confirms the findings cited in a previous paper discussing initial results of simple shear testing as applied to polycarbonate (Gopez, 1984).

Discussion

Review of Previous Shear Band Studies with Different Modes of Deformation

Deformation bands in amorphous polymers have already been observed in compression (Whitney, 1963; Argon et al., 1968; Bowden and Raha, 1970), tension (Bauwens, 1967 and 1970; Brady and Yeh, 1971) and in torsion testing (Bauwens, 1970, Wu and Turner, 1973). Polymers studied were polystyrene (PS), polymethylmethacrylate (PMMA), polyvinyl chloride (PVC) and polycarbonate (PC).

In tension testing, the observed deformation bands are inclined with respect to the stress axis and their appearance precedes the onset of necking. The study of these bands, however, has been hindered by crazes which form together with the bands and subsequently cause rupture. These bands have been compared to Luders bands (Pomey et al., 1964) which have been observed in metals.

In compression, the deformation bands initiate at points of stress concentration (a crack or defect, for example). By putting markers on the specimen surface, it has been shown by several workers (Argon et al., 1968; Wu and Li, 1976) that deformation in these bands takes place by shear. For specimens of rectangular cross-section two perpendicular sets of bands have been observed (Argon et al., 1968). The interaction of these sets of bands makes the analysis of the phenomenon difficult (Bowden and Raha, 1970). Under certain conditions (i.e., polished specimen edges, use of a notch situated close to a specimen end, etc.) it is possible to suppress one of these sets of bands and study only one set propagating into the specimen. Wu and Li (1976) and later Chau and Li (1979, 1980, 1981, 1982a and b) have been able to make detailed studies of such bands in polystyrene. These researchers found two types of bands at ambient temperature: coarse bands and fine bands (Wu and Li, 1976). The latter appear to be diffuse shear zones (Bowden and Raha, 1970; Kramer, 1974) to the naked eye and only electron microscopy has revealed the presence of fine bands in these zones. The predominance of one type of band over the other seems to be related to temperature effects. Bowden

and Raha (1970) found a transition between diffuse zone deformation (actually fine bands) which takes place at high temperatures and (coarse) band deformation which takes place at low temperatures (very much lower than T_g). In the case of PMMA, coarse bands form only at very low (sub-zero) temperatures while the diffuse zones predominate at ambient temperatures (Whitney and Andrews, 1967). Shear bands obtained in compression have high propagation speeds which can attain 185 mm/s (Chau and Li, 1982a). For a small specimen (25 mm long, 9 mm wide), the bands traverse the sample in less than 0.20 seconds. High speed photography must be used to study these deformation bands. The bands have also been shown to widen during propagation but this phenomenon is difficult to study (Wu and Li, 1976) due to the short time interval in which it occurs.

In torsion, the observed shear bands develop and spread more slowly. Their evolution is similar to that found for bands in simple shear testing: the band elongates and then widens (Wu and Turner, 1973). However, the state of stress to which the specimen is subjected is rather complex and may make the analysis of the phenomenon difficult. One particular problem arises from the difficulty with which a moment vs angle of rotation curve may be transformed into a shear stress vs shear strain curve (Canova et al., 1982; Shrivastava et al., 1982). The cylindrical form of the torsion specimen also makes observation of the entire shear band difficult.

Characterization of Deformation Bands in Simple Shear

In contrast to the bands observed in other testing modes, bands obtained in simple shear testing are generally free from parasite effects such as crazing or band intersection. Only one band usually forms and propagates, initially by elongation and then by widening. The band axis is parallel to the shear stress axis. Observations carried out on modified specimens with surface markers indicate that material in the band is deformed by shear, the same mode of deformation as that applied macroscopically to the specimen.

No variation of specimen dimensions in the region occupied by the shear band has been observed. Measurements done with a Tesa profilometer on a specimen with a 2.04 mm-wide (h_B) shear band (with a plastic shear strain of 0.60, Stage III) showed that the area occupied by the band was thinner by only 0.4%. This decrease in volume was confirmed by corresponding density increases in the deformed material (Gopez, 1984).

Simple shear testing seems to produce a "pure" phenomenon of plastic instability because (as opposed to necking of tensile test specimens) there is little or no change in the cross-sectional area of the deformed zone. Therefore, the same stress acts on the shear band and on the undeformed adjacent regions in the specimen's calibrated part. These two regions in the specimen have two distinct values of shear strain for the same shear stress.

Shear Band Kinetics

General Analysis

As a first approximation the shear strain in a test specimen can be expressed as:

$$\gamma = \gamma_{el} + \gamma_{pl}$$

where γ_{el} is the elastic deformation and γ_{pl} is the non recoverable plastic deformation component. It has been shown that all of the plastic strain is concentrated in the shear band. Using shear band parameters we can write:

$$\gamma_{pl} = (x_B/h)\,(L_B/L)$$

where x_B = displacement in the shear band
h = sheared width (in this case equal to the width of the specimen's calibrated part)
L_B = length of the shear band
L = specimen length.

This relationship may also be expressed as a function of the shear strain in the band γ_B ($=x_B/h_B$ where h_B is the width of the band, Figure 7). We have:

$$\gamma_{pl} = \gamma_B\,(h_B/h)\,(L_B/L)$$

The shear strain rate can be written as:

$$\dot{\gamma} = \dot{\gamma}_{el} + \dot{\gamma}_{pl}$$

Developing the expression for $\dot{\gamma}_{pl}$ gives:

$$\dot{\gamma} = \dot{\gamma}_{el} + \gamma_B(h_B/h)\,(\dot{L}_B/L) + \gamma_B(L_B/L)\,(\dot{h}_B/h) + (L_B/L)\,(h_B/h)\dot{\gamma}_B$$

Figure 8 shows the contribution of the four terms of the shear strain rate equation during the different deformation stages. In Stage I no band is visible and all strain is recoverable. The first term of the strain rate equation gives the total strain at this stage ($\dot{\gamma} = \dot{\gamma}_{el}$).

During Stage II, the predominant factor is the elongation rate $\dot{L}$ of the band. The steep slope of the L_B/L curve in Figure 8 confirms this. The second term of the strain rate equation, $\gamma_B(h_B/h)\,(L_B/\dot{L})$ thus becomes the contributing term. At the end of Stage II, L_B no longer changes and $\dot{L}_B$ becomes zero. Band widening now becomes more significant and the third term, $\gamma_B(L_B/L)\,(\dot{h}_B/h)$ should represent what happens in Stage III.

In Stage IV $\dot{L}_B$ and $\dot{h}_B$ are both zero and only the strain rate in the band $\dot{\gamma}_B$ contributes to the plastic strain rate. The last term of the strain rate equation defines this stage.

Internal Stress of the Specimen in Stage II

The existence of localized plastic strain gradients at the shear band tips induces internal stresses in the specimen. These stresses must be concentrated at the shear band ends but would not be due to a change in specimen cross-sectional area. Rather, these would be due to the shear band itself.

These stresses were estimated using two methods:

(i) By theoretical calculations based on the concept of a pile-up of infinitesimal dislocations (this method is also used by geologists to predict the internal stresses at the tip of a shear fissure in a rock mass)

(ii) By photoelasticity

The stress concentration at the shear band tip is due to the previously described transition region (Figures 5 and 11a) at a shear band tip. This transition cannot be obtained without producing a stress field at the shear band tip. To calculate this stress the strain gradient at the band tip may be considered to be a dislocation pile-up (Figures 11b and c) with a Burgers vector $\beta(x)dx$ (Li, 1982) such that:

$$\beta(x) = \frac{d\,\delta x_B}{dx}$$

where δx_B is the displacement at a point in the band tip.

If the shear strain is assumed to be distributed throughout the shear band front, the maximum shear strain in the band will be:

$$B = X_B = \int_{-\ell/2}^{+\ell/2} \beta(x)dx$$

The shear stress resulting from such a strain distribution is given by the expression:

$$\tau(x) = \int_{-\infty}^{+\infty} \frac{\mu\beta(x')dx'}{2\pi(1-\upsilon)} \frac{1}{(x-x')} \simeq \int_{x=-\ell/2}^{+\ell/2} \frac{\mu\beta(x')dx'}{2\pi(1-\upsilon)} \frac{1}{(x-x')}$$

where $\tau(x)$ = shear stress at point x.

The appropriate function β_m corresponding to the shear strain gradient at the shear band tip must now be chosen. The details of the solution are given in the Appendix.

The β_m function represented on Figure 12 was found to best fit the data obtained in Figure 5. The transition region has a central portion of length z in which the shear strain gradient is constant and end zones each measuring $(\ell - z)/2$ in length.

The internal shear stress τ_T produced at the band tip is now given by the following expressions:

$$\tau_T = \frac{A}{(1-\alpha)}\left[\left(1+\frac{2x}{\ell}\right)\ln\left(1+\frac{\ell}{2x}\right) - \left(\alpha+\frac{2x}{\ell}\right)\ln\left(1+\frac{\alpha\ell}{2x}\right) + \left(\alpha-\frac{2x}{\ell}\right)\ln\left(1-\frac{\alpha\ell}{2x}\right) - \left(1-\frac{2x}{\ell}\right)\ln\left(\frac{\ell}{2x}-1\right)\right]$$

$$\text{for } \frac{z}{2} < x < \frac{\ell}{2}$$

$$\text{and } \tau_T = \frac{A}{(1-\alpha)}\left[\left(1+\frac{2x}{\ell}\right)\ln\left(1+\frac{\ell}{2x}\right) - \left(\alpha+\frac{2x}{\ell}\right)\ln\left(1+\frac{\alpha\ell}{2x}\right) + \left(\alpha-\frac{2x}{\ell}\right)\ln\left(\frac{\alpha\ell}{2x}-1\right) - \left(1-\frac{2x}{\ell}\right)\ln\left(\frac{\ell}{2x}-1\right)\right]$$

$$\text{for } 0 \leq x \leq \frac{z}{2}$$

$$\text{with } A = \frac{\mu\beta m}{2\pi(1-\upsilon)}, \quad \beta m = \frac{2B}{\ell(1+\alpha)}, \quad \alpha = \frac{z}{\ell}$$

Figure 13 shows the variation of the stress τ_T in region around the band tip. The maximum value of τ_T can be found between $x = z/2$ and $x = 1/2$ in the transition region. This is actually at the tip of the band. Using $\mu = 820$ MPa, $\upsilon = 0.4$, $\ell = 4$mm, $B = 75\ \mu$m and $z/\ell = 0.8$, the value obtained for $\tau_{T\,max}$ is 45.2 MPa. This is approximately 15 percent higher than the applied stress which forms the shear band at the beginning of Stage II.

In this preceding calculation only the stress due to the shear strain gradient in the shear band tip has been taken into consideration. The long range stresses due to the strain gradient in the other shear band tip must also be included in the calculations (Kramer, 1975; Chau and Li, 1981). The dislocation analogy can still be used but this time because of the distance between the tips, it will no longer be necessary to consider a distribution of infinitesimal dislocations at each tip. The case of an edge dislocation dipole (Figure 14) will be considered and the shear stress produced on one shear band tip by the other is simply:

$$\tau_D = \frac{-\mu B}{2\pi(1-\upsilon)} \frac{1}{L_B}$$

The negative sign indicates that this stress acts in a sense opposite to that of the applied stress and opposite to the positive stress peak (in Figure 13) due to the shear strain gradient. Using the values, μ = 820 MPa, υ = 0.4, B = 75mm (obtained from Figure 5), $\tau_D = 16.3/L_B$ where τ_D is in MPa and L_B is in mm. It is to be noted that τ_D is inversely proportional to the length of the band. The shear stress τ_D is significant when the band is short (τ_D - 3.3MPa for L_B = 5mm) and gradually diminishes when the band becomes longer. This stress can be interpreted to be a reciprocal attraction force between the shear band tips which are taken to behave like a dipole of edge dislocations with Burgers vectors of opposite signs $-B$, $+B$ (Figure 14).

The total stress at a point in the specimen will therefore be the sum of the applied stress and the internal stresses τ_T and τ_D produced at and by the shear band tips. In the plane containing the band, Figure 15 shows that the shear stress distribution curve has a peak in front of each shear band tip. These regions of high stress lead to localized deformation and to the propagation (elongation) of the shear band.

To demonstrate the stress concentration at each end of the band, a specimen deformed up to the beginning of Stage II was polished and examined in a polariscope. From this photoelastic analysis, the direction of the prevailing principal stresses can be obtained from the isoclines, and the value of the difference in principal stress ($\sigma_1 - \sigma_2$) may be calculated from the isochromes (Frocht, 1941; Robert, 1970). An isocline represents the locus of points of optical extinction at which the principal stress directions are parallel to the optical axes of the polarizers. Isoclines are black in both monochromatic and polychromatic (or white) light. An isochrome passes through points with the same maximum shear stress (and the same difference in principal stresses). In white light, the dispersion of colors makes isochromes

black (zero order, zero maximum shear stress) or different colors (higher orders). In monochromatic light the fringes (isochromes) are white or black. The number of black fringes (which corresponds to the order given by the tint of passage in white light) allows the calculation of the stress at a given point by the relation:

$$\Delta\sigma = \frac{n\lambda}{Ce}$$

where C = coefficient of photoelastic sensitivity of the material

λ = wave length of the light used

e = specimen thickness

n = number of fringes (or orders)

The coefficient C of polycarbonate was determined in tension to be 8.54 10^{-5} MPa^{-1}.

In Figures 16 a and b, photographs taken at different orientations of the shear band with respect to the optical axis of the polarizers (vertical in this case) show that the isoclines change in appearance with the orientation. The diagram in Figure 16c shows three of the isoclines observed (at increments of 30° in the orientation). Eight points of intersection (singular points) can be observed on either side of the shear band. Since the principal stresses cannot possibly have all of the orientations at a single point, these points must be points of zero principal stresses.

Figure 16d, taken with quarter wave plates oriented at 45° with respect to the polarizer's optical axis, shows only the isochromes. The singular optical points are immediately seen to be occupied by black isochromes, thus further supporting the conclusion that they must be points of zero stress. These points must also be of zero order. Starting from one of these points (the one above and to the left of the band for example) and going towards the shear band tip, three fringes can be seen with the last one close to the band tip. The stress at this point is therefore:

$$\Delta\sigma = \frac{n\lambda}{Ce} = 8.1 \text{ MPa}$$

with λ = 5650 A°(white light)

e = 2.40m

n = 3

This verifies the existence of a stress at the band tip. The measured value is lower than that calculated for by using the dislocation pile-up model. It is quite possible that the real stress is actually greater than the value cited above. The other fringes may not be visible due to the limit of resolution of the method used.

Plastic Flow at the Band Tip

The plastic deformation of the material at the shear band tip is due to three essential factors:

a) multiplication of internal structure defects

b) high local shear strain rate

c) stress due to macromolecular orientation

In a previous article (Gopez, 1984) the concept of elementary microscopic defects linked to the mechanism of plastic deformation was introduced. If one of these defects produces an elementary shear displacement b, and if their density is ρ, then assuming these defects to propagate at a velocity v, enables an estimation of the plastic shear strain rate by using Orowan's equation:

$$\dot{\gamma}_{pl} = \rho b v$$

In an annealed undeformed specimen, the initial defect density ρ_i may be considered to be small such that a given strain rate may not be imposed until one of the following conditions is satisfied:

(i) a rapid increase in the number of defects in order to raise the value of ρ

(ii) an increase in the shear stress to produce a very high value of v.

The first condition cannot be satisfied instantaneously because it can be shown (Gilman and Johnston, 1962; Johnston, 1962; G'sell and Jonas, 1981) that the multiplication of defects requires the accumulation of a certain amount of plastic deformation. It is therefore understandable that plastic deformation is localized and concentrated in a shear band because the local stress at the band tip (τ_T) allows the needed increase in v during the time in which the number of defects increases slowly. The local stress concentration does not require a very high value of the applied stress. By the same argument it can be explained why the plastic deformation at high temperatures or of specimens subjected to a plastic deformation cycle ("cycled specimen") is homogeneous. In the "cycled specimens" the initial defect density ρ_i is already high enough and uniform enough in the whole specimen to allow immediate plastic flow without a high value of applied stress. At high temperatures, the mobility of the molecular chains is such that the defects form rapidly without high energy barriers to be overcome by additional stress.

It will be shown, however, that localized plastic deformation requires local strain rates which are actually higher than the imposed nominal strain rate.

In the plane of the band, an element of material is subjected to a high strain rate at the instant that it is reached by the shear band tip (shear band front). As a first approximation approach, the local shear strain gradient $d\gamma/dx$ at the band tip can be assumed to be linear and the rate at which the band elongates can be designated by $\dot{L}$. The instantaneous strain rate can be expressed as:

$$\dot{\gamma}_T = \frac{d\gamma}{dt} = \frac{d\gamma}{dx} \cdot \frac{dx}{dt}$$

$$= \frac{\gamma_B}{\ell} \cdot \frac{\dot{L}_B}{2}$$

where ℓ is the length of the shear band front.

For deformation in Stage II we previously obtained the expression that

$$\dot{\gamma} \simeq \dot{\gamma}_{pl} \simeq \frac{h_B}{h} \gamma_B \frac{\dot{L}_B}{L}$$

Combining the two strain rate expressions gives:

$$\dot{\gamma}_T = \frac{\dot{\gamma}}{2} \frac{L}{\ell} \frac{h}{h_B}$$

where $\dot{\gamma}$ is the nominal imposed strain rate.

For ℓ= 4mm, L = 60mm, h_B = 0.1 and h = 4mm, the local shear strain rate at the band tip is equal to:

$$\dot{\gamma}_T = 300\,\dot{\gamma}$$

Knowing that the strain rate sensitivity coefficient of the material (Gopez, 1984), $m = \partial \ln\tau / \partial \ell n\dot{\gamma} = 0.03$, $\tau(\dot{\gamma}_T, \gamma)$ is found to be 20% higher than $\tau(\dot{\gamma}, \gamma)$. A part of the stress concentration at the band tip is therefore used to give the extra stress needed to produce the high local strain rate.

The deformation of macromolecular chains under the action of a given shear stress is limited by a restoring stress which tends to return the chains oriented by the applied external stress to their initial random and isotropic configuration. This effect certainly differentiates an amorphous polymer from an amorphous metal. In the latter, slip can take place without strain hardening and the deformed metal cannot recover its initial configuration and dimensions by annealing. In the case of polycarbonate, the strain hardening observed in shear testing during the steady state plastic deformation regime (Stage IV or "cycled specimen") may be taken to correspond to the macromolecular chain orientation effect. Material in a shear band deformed up to $\gamma_{B\,pl}$ is then subjected to an internal stress due to molecular orientation:

$$\tau_{or} = \left(\frac{\partial \tau}{\partial \gamma}\right)_{\dot{\gamma}} \cdot \gamma_B$$

At 23 °C, $\partial\tau/\partial\gamma$ = 20 MPa which gives $\tau_{or} = -10$ MPa for $\gamma_B \simeq 0.5$.

All of the stresses affecting plastic strain at a band tip during Stage II may now be taken into consideration:

$$\tau^*(\dot{\gamma}_T, \rho_i) + \tau_{or}(\gamma_B) = \tau_a + \tau_T + \tau_D(L_B)$$

The left side of the equation gives the additive form of the expression for the total flow stress of the polymer at the shear band tip. The right side gives the sum of the applied stress and the internal stresses due to the shear band tips. The total applied stress needed may be obtained by rewriting the expression:

$$\tau_a = \tau^*(\dot{\gamma}_T / \rho_i) + \tau_{or}(\gamma_B) - \tau_T - \tau_D(L_B)$$

During the elongation (extension) of the band, each of the terms remains constant except for τ_D whose absolute value decreases as the length of the band increases. This decrease $-\tau_D$ seems to be the reason for the stress drop after yield on the stress-strain curve. The magnitude of the stress drop ($\simeq$ 3 MPa) would indicate that the band would be about 5mm long at the moment of its formation.

Widening of the Band (Stage III)

In Stage III the shear test specimen contains two zones in its calibrated part which have different strains but are under the same stress. Beside the deformed material in the shear band will be found totally undeformed material. The same stress applies to both regions because there is no change in cross-sectional area which could result in a stress concentration.

No detailed mechanism of shear band widening in glassy amorphous polymers has been proposed to date. For crystalline metals the widening of Luders bands and shear bands in general has been explained by cross slip mechanisms (Pomey, et al., 1964; Friedel, 1964). In polymers the widening of deformation bands in polycarbonate deformed in torsion has been observed by Wu and Turner (1973) but they did not offer a detailed analysis nor advance a mechanism.

The defect theory may provide a mechanism for band widening. The premises of the mechanism are:

a) nucleation of defects is more difficult than their movement (or migration)

b) a plastically deformed zone contains the critical defect density.

Acceptance of these two premises leads to the statement that the applied external stress makes the existing defects in the shear band migrate towards the undeformed zones and results in an increase of the local defect density in regions near the band interface. It is also possible that the arrival of migrating defects may trigger more nucleation. In this way, the critical defect density is more rapidly attained at the interface and the shear band widens. This takes place at a stress lower than that needed to start another band ($\tau_{apl} = \tau_{min}$ of stress drop). At this stress level, nucleation of defects is difficult and the formation of another band elsewhere in the calibrated portion of the specimen cannot take place. Widening then becomes the favored mechanism for continued plastic deformation.

At the beginning of Stage III, $L_B = L$ and $\dot{L}_B$ becomes zero. The strain rate is now expressed as:

$$\dot{\gamma} \simeq \dot{\gamma}_{pl} \simeq \gamma_B \left(\dot{h}_B/h\right) + \left(h_B/h\right) \dot{\gamma}_B$$

The term containing $\dot{h}_B$, γ_B $(\dot{h}_B/h)$ is important at the start of Stage III while the homogeneous deformation term becomes predominant at the end.

The factors affecting the widening of the band will now be discussed:

a) widening stress

This must be equal to the applied stress τ_a. Under the action of this stress, widening of the band must take place without any stress concentration.

b) macromolecular chain orientation stress (τ_{or})

In the same manner as in Stage II, this stress is due to strain hardening and may be expressed as $\tau_{or} = (\partial\tau/\partial\gamma)_{\dot{\gamma}} \cdot \gamma_B$. The shear strain γ_B in the band increases slowly in Stage III and consequently τ_{or} must also increase.

c) strain rate effects

Additional stress τ_s may be needed to make the material at the band interface deform rapidly and contribute to the widening. To calculate τ_s, the strain rate $\dot{\gamma}_i$ at the advancing band interface must be calculated. Figure 17 shows a band interface as seen on a specimen with markers. The variation of the shear strain γ along an axis y perpendicular to the shear axis x is represented in Figure 18. In the same manner as for a band tip, a characteristic dimension of this

interface may be defined as w. In this region, the shear strain varies from zero (undeformed material) to γ_B (material in the band).

The local strain rate $\dot{\gamma}_i$ at the interface is given by the relationship:

$$\dot{\gamma}_i = \frac{\partial \gamma}{\partial t} = \frac{\partial \gamma}{\partial y} \frac{\partial y}{\partial t} = \frac{\gamma_B}{w} \cdot \frac{\dot{h}_B}{2}$$

But

$$\dot{h}_B \simeq \frac{h}{h_B} \left(\dot{\gamma} - \frac{h_B}{h} \dot{\gamma}_B \right)$$

Assuming the second term in the parentheses to be negligible, this expression reduces to:

$$\dot{h}_B \simeq h (\dot{\gamma}/\gamma_B)$$

and this gives:

$$\dot{\gamma}_i = \frac{1}{2} \frac{h}{w} \dot{\gamma}$$

Since w is very small the strain rate $\dot{\gamma}_i$ of the material at the band interface is very much higher than the nominal imposed strain rate $\dot{\gamma}$ during the test. Due to this strain rate difference, it is necessary to apply an extra stress τ_s for widening to take place. If h/w = 50 (w = 0.08mm), then $\dot{\gamma}_i = 25\dot{\gamma}$ and since $\tau(\dot{\gamma}_i)/\tau(\dot{\gamma}) = (\dot{\gamma}_i/\dot{\gamma})^m$ this gives $\tau(\dot{\gamma}_i, \gamma) = 1.1\ \tau(\dot{\gamma}, \gamma)$.

In order to explain the evolution of the shear-strain curve in Stage III, the level of stress needed to give the same strain at the same local strain rate in the absence of shear band must be known. The test curve of a "cycled specimen" (curve 2, Figure 19) could furnish this information since the whole specimen is already uniformly deformed at the start of the test.

The shape of the stress-strain curve in Stage III may now be explained. In particular, it must be explained why the stress increases slowly in this stage instead of remaining constant as in the case of Luders band propagation. To answer this question the construction of Figure 19 will be used. The plastic shear strain $\gamma_{B\,pl}$ increases slowly in Stage III and Figure 20 shows the variation of $\gamma_{B\,pl}$ with total shear strain ($\gamma = \gamma_{el} + \gamma_{pl}$).

Consider a point on the $\tau - \gamma$ curve which is in Stage III, $\gamma = 0.27$. From Figure 20, $\gamma_{B\,pl} = 0.67$. This value was obtained for the unloaded specimen, and to get the total strain (under charge), the elastic strain γ_{el} must be added to 0.67. Figure 21 provides a direct reading correction curve which gives γ_B total = 0.87. The corresponding stress needed to have this total strain is now obtained from the curve for the "cycled specimen" (τ = 32.6 MPa Figure 19). This is compared with the corresponding stress at the corresponding point on the τ–γ curve, (τ = 35.6 MPa). The difference between these two values is due to the high value of the local shear strain rate. This can be calculated: $(\dot{\gamma}_i/\dot{\gamma})^m = \tau(\gamma, \dot{\gamma}_i)/\tau(\gamma,\dot{\gamma})$. This gives $\dot{\gamma}_i = 19\ \dot{\gamma}$ implying that h/w = 19 and w = 0.095mm. This value for w is in good agreement with the value obtained (0.08mm) by measuring the width of the lateral transition zones in photographs of specimens.

It can now be said that during widening, the observed stress is essentially affected by:

a) the plastic shear strain in the band, $\gamma_{B\,pl}$

b) the local shear strain rate which depends in turn on the local shear strain gradient at the band interface

Homogeneous Deformation (Stage IV)

In Stage IV, the strain rate is simply written as

$$\dot{\gamma} = \dot{\gamma}_{cl} + \dot{\gamma}_B$$

because $L_B = L$, $\dot{L_B} = 0$ and $h_B = h$, $\dot{h_B} = 0$. However, it seems that h_B while having a very small value still continues to have an effect. Consequently the local strain rate at the band edges may still be high and this may explain the vertical offset between the two curves in Figure 19 during Stage IV. This offset decreases up to the end of the test and this signifies that $\dot{h}_B$ decreases as the shear band spreads into the specimen grips.

During this stage, deformation continues by an increase in γ_B. The strain hardening mechanism becomes more significant and the slope of the $\tau-\gamma$ curve becomes steeper.

The deformation at this stage is apparently homogeneous. On the molecular scale, however, the nucleation and movement of elementary microscopic defects must continue to take place. The defect density may be considered to remain constant throughout Stage IV and the prevailing density will be characteristic of the imposed strain rate $\gamma_{B\,pl}$ (G'sell and Jonas, 1981).

Temperature Effects

The plastic deformation model just discussed may also be used to interpret the effects of temperature on the intrinsic mechanical response of polycarbonate in simple shear.

At low temperatures, multiplication of defects requires a very high stress due to the small amount of available thermal energy. A stress peak of high amplitude is then to be expected at yield. The strain hardening coefficient as shown by the slope of the stress-strain curve after the yield point will be high (or steep) because of the low mobility of molecular chains in this temperature range. This predicted response is represented in the form of the intrinsic stress-strain curve of the material (local true shear stress vs local true shear strain) in Figure 22 (curve T_1). With such a material response, if the stress is maintained at the maximum of the stress peak at yield, the strain should stabilize at a low value γ_{m1}.

At high temperatures (T_3 close to T_g), the nucleation of defects is easier and does not require an overstress (only a small stress peak is needed at yield). The strain hardening coefficient is likewise small because of the rubbery behavior of the material at this temperature. The strain γ_{m3} corresponding to the maximum stress at yield will be small but not for the same reasons as at low temperatures.

At intermediate temperatures ($T_2 \simeq T_{amb}$ for example) the stress peak and strain hardening coefficients should take on intermediate values. The resulting stabilized strain at the stress peak γ_{m2} should be relatively large.

Considering this *intrinsic* behavior the results of a shear test may now be understood. The formation of a shear band is favored by a high intrinsic yield stress peak *and* a low subsequent strain hardening coefficient. This makes the phenomenon more observable at intermediate temperatures. The system favors a configuration with two strain levels (localized plastic deformation) to homogeneous deformation. At low temperatures the band tends to form but the strain hardening rate is so high that the whole specimen must be deformed. Around T_g the defects multiply rapidly in the whole specimen and the band has no tendency to form.

Conclusion

Shear band formation in polycarbonate deformed in simple shear has been extensively studied. Results show the formation and propagation of a single shear band. The stages of formation and propagation can be correlated with the shear stress (τ) vs. shear strain (γ) curve.

The absence of cross-sectional change in test specimens showed that shear band appearance was not due to mechanical stress concentration effects. Shear band elongation was shown to be due to a stress at the shear band tip induced by the strain gradient and the interaction with the other band tip. Part of this stress was needed to produce a local strain rate very much higher than the nominal strain rate.

A mechanism of shear band widening was proposed. The basis was a defect theory of plastic deformation previously proposed by a number of investigators. The tendency to have heterogeneous plastic deformation was accounted for by the same defect theory.

The observations done on "cycled specimens" verified that plastic deformation was immediately homogeneous and that no new shear bands were formed in these specimens.

The end effects were also investigated using specimens with surface markers. Results confirmed previous observations obtained for sheared polycarbonate.

REFERENCES

ARGON A.S., ANDREWS R.D., GODRICK J.A. and WHITNEY W. (1968), J. Appl. Phys., 39, 1899.

BAUWENS J.-C. (1967), J. Polym. Sci. A-2, 5, 1145.

BAUWENS J.-C. (1970), J. Polym. Sci. A-2, 8, 893.

BONI S. (1981), "Conception d'une Machine de Cisaillement Plan pour la Determination du Comportement Plastique de Materiaux Polymeres", These d' Ingenieur C.N.A.M., NANCY.

BOWDEN P.B. and JUKES J.A. (1968), J. Mater, Sci., 3, 1833.

BOWDEN P.B. and RAHA S. (1970). Phil. Mag., 22, 463.

BRADY T.E. and YEH G.S.Y. (1971), J. Appl. Phys., 42, 4622.

CANOVA G.R., SHRIVASTAVA S., JONAS J.J. and G'SELL C. (1982), " The Use of Torsion Testing to Assess Material Formability" in "Formability of Metallic Materials-2000 A.D.", ASTM STP 753, J.R. NEWBY and B.A. NIEMEIER ed., American Society for Testing and Materials, p. 189.

CHAU C.C. and LI J.C.M. (1979), J. Mater. Sci., 14, 1593.

CHAU C.C. and LI J.C.M. (1980), J. Mater. Sci., 15, 1898.

CHAU C.C. and LI J.C.M.(1981), J. Mater. Sci., 16, 1858.

CHAU C.C. and LI J.C.M. (1982)A, J. Mater. Sci., 17, 652.

CHAU C.C. and LI J.C.M. (1982)B, J. Mater. Sci., 17, 3445.

FROCHT M. (1941), "Photoelasticity" Vol. I, John Wiley and Sons, Inc., New York.

GOPEZ A.J.R. (1983), "Etude de la Deformation du Polycarbonate en Cisaillement Simple" Thesis "Docteur-Ingenieur", INPL, Nancy, France.

GOPEZ, A.J.R. (1984), Phil. Eng'g Journal, V, 1.

G'SELL C. and JONAS J.J. (1981), J. Mater. Sci., 16, 1956.

G'SELL C., BONI S. AND SHRIVASTAVA S. (1983), J. Mater. Sci., 18, 903.

G'SELL C. and GOPEZ A.J.R. (1984), J. Mater. Sci., submitted for publication.

KRAMER E. J. (1974), J. Macromol. Sci., B10,1, 191.

LI. J.C.M. (1982), "Dislocation Theory" and "Internal Stresses" in "Plastic Deformation of Amorphous and Semi-Crystalline Materials", B. ESCAIG, and C. G'SELL ed., Editions de Physique.

POMEY G., GRUMBACH M. et CRUSSARD C. (1964), Mem. Sci. Rev. Met., 4, 243.

ROBERT A. (1970), "Polarimetrie et Photoelasticimetrie", Cours E.N.S.T.A., Paris.

SHRIVASTAVA S., JONAS J.J. and CANOVA G. (1982), J. Mech. Phys; Solids, 30, 75.

VISHAY MICROMESURES, "Manuel d' Analyse Experimentale des Contraintes", Paris.

WHITNEY W. (1963), J. Appl. Phys., 34, 3633.

WHITNEY W. and ANDREWS R.D. (1967), J. Polym. Sci., C16, 2981.

WU J.B.C. and LI J.C.M. (1976), J. Mater, Sci., 11, 434.

WU W. and TURNER A.P.L. (1973), J. Polym. Sci., Polym. Phys. Ed., 11, 2199.

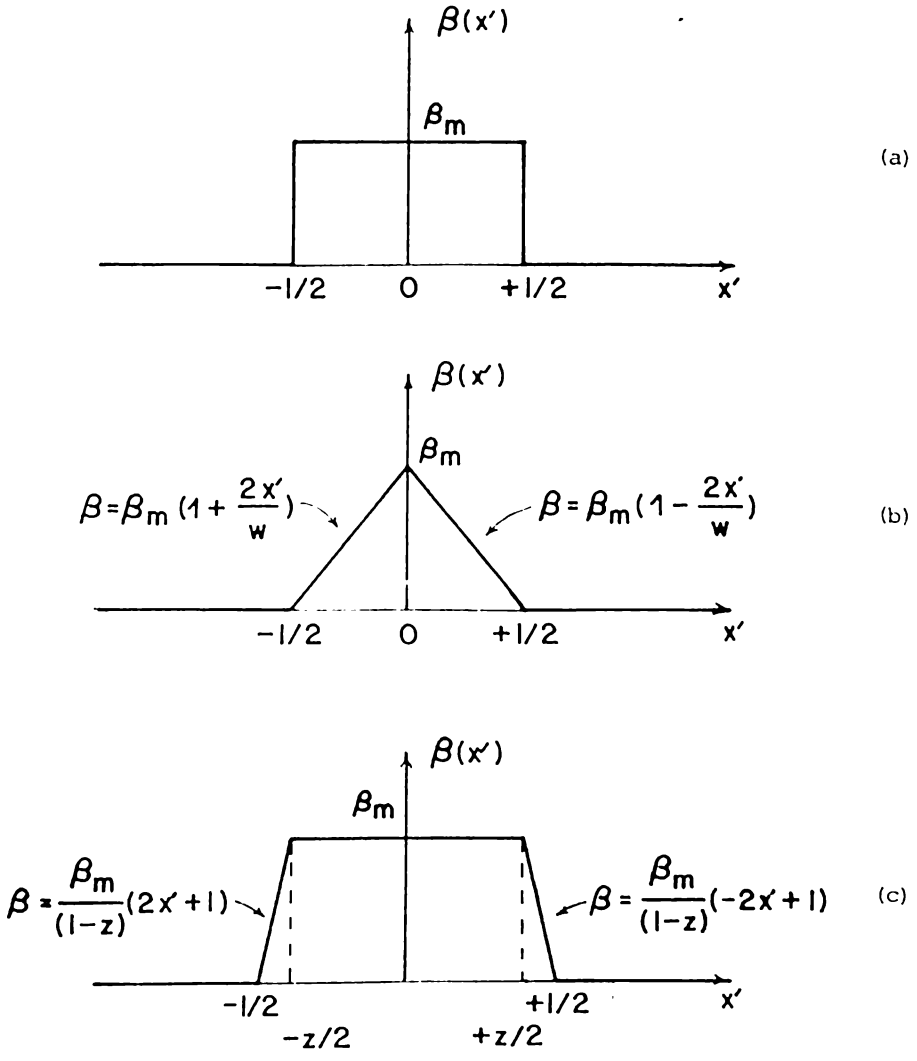

Figure A1: Forms of $\beta(x')$

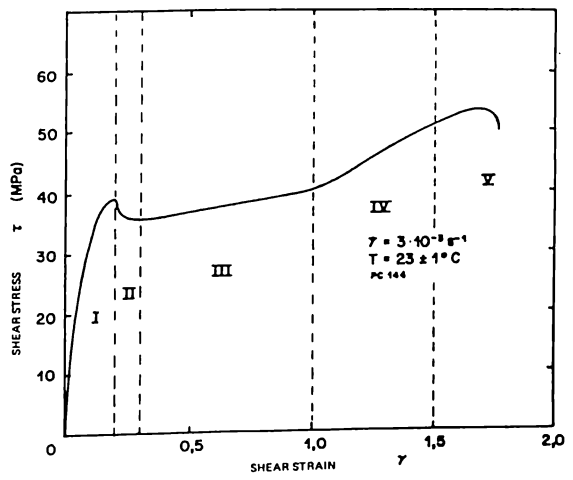

Figure 1. Typical shear stress – shear strain curve for polycarbonate, from Gopez (1984), Figure 7.

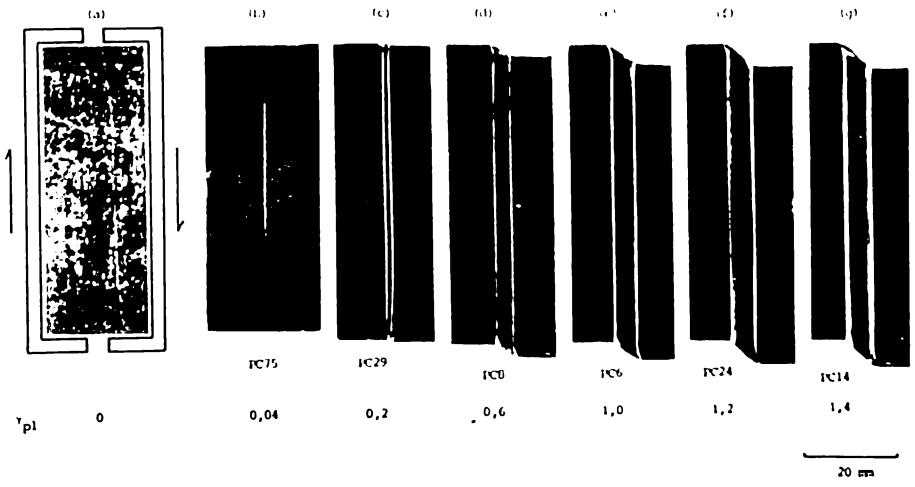

Figure 2. Shear band formation and development in polycarbonate from Gopez (1984), Figure 15.

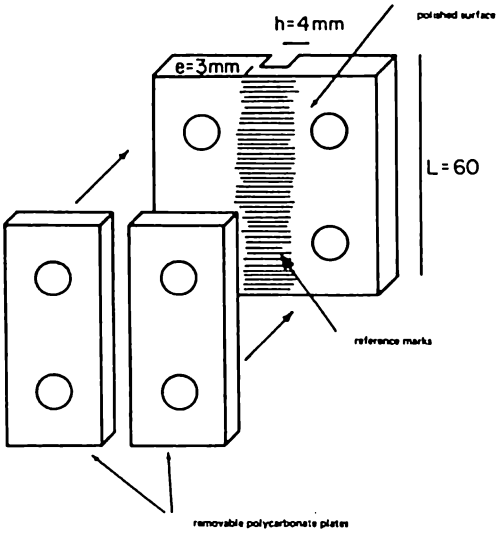

Figure 3a. Test specimen modified to put reference marks on the surface of the calibrated part.

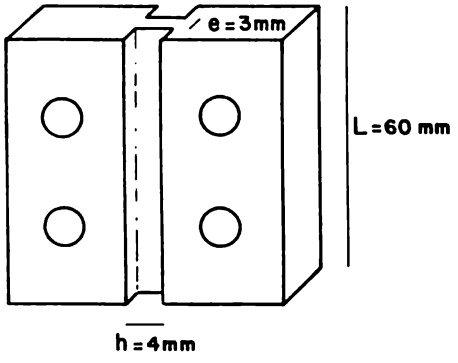

Figure 3b. Conventional specimen.

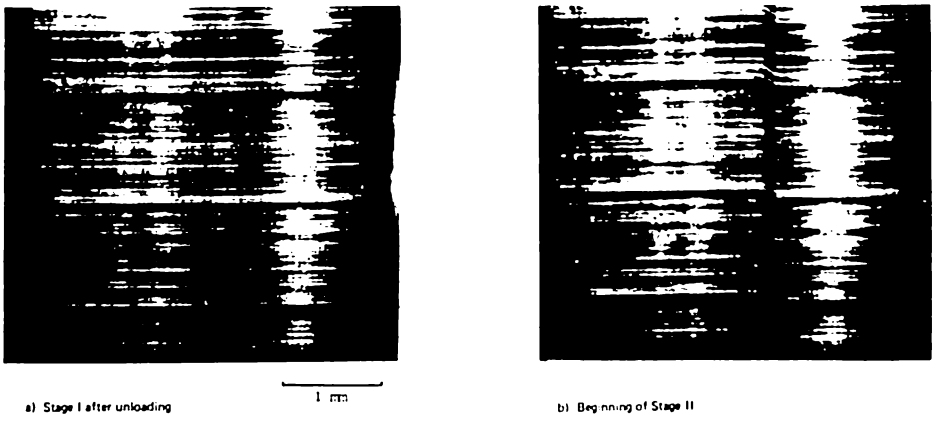

Figure 4. Evolution of the shear band during a simple shear test shown by reference marks on a modified specimen (PC 133).

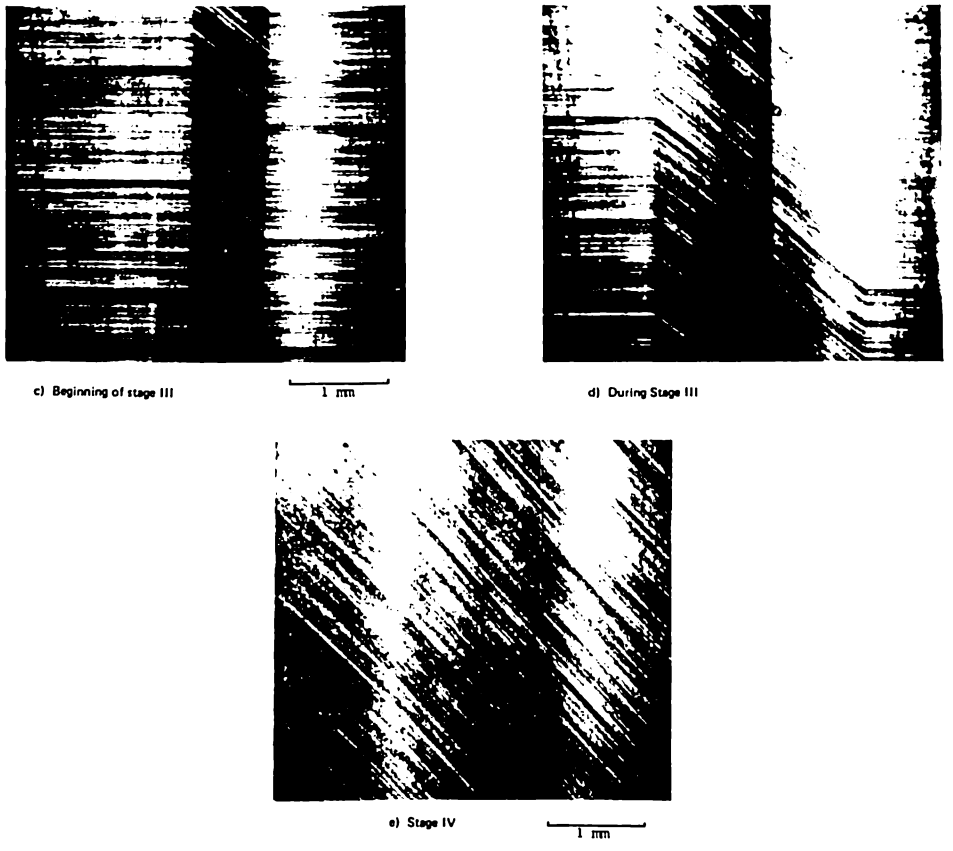

Figure 4. Evolution of the shear band during a simple shear test shown by reference marks on a modified specimen (PC 133).

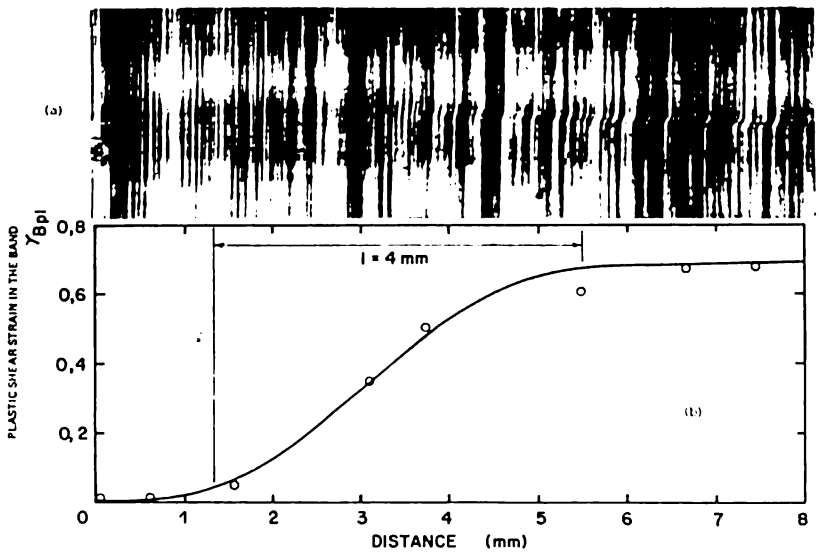

Figure 5. a) Shear band at the beginning of Stage III (PC 133).
b) Variation of local plastic shear strain at the band tip.

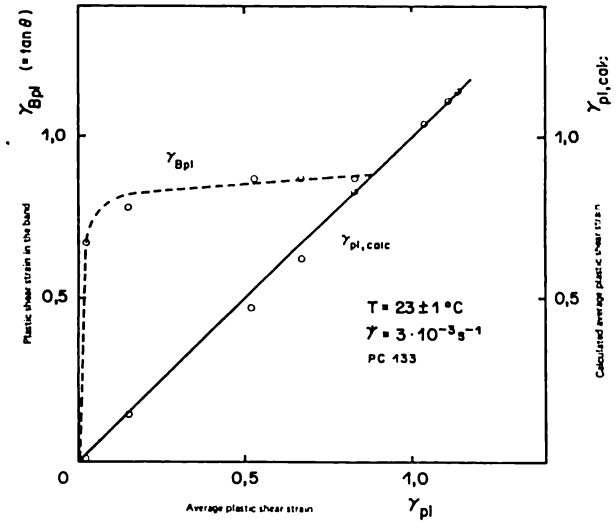

Figure 6. Plastic shear strain in the band and calculated average plastic shear strain composed with measured average plastic shear strain.

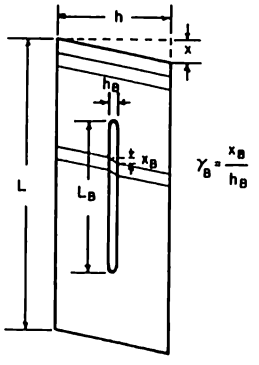

Figure 7. Shear band parameters.

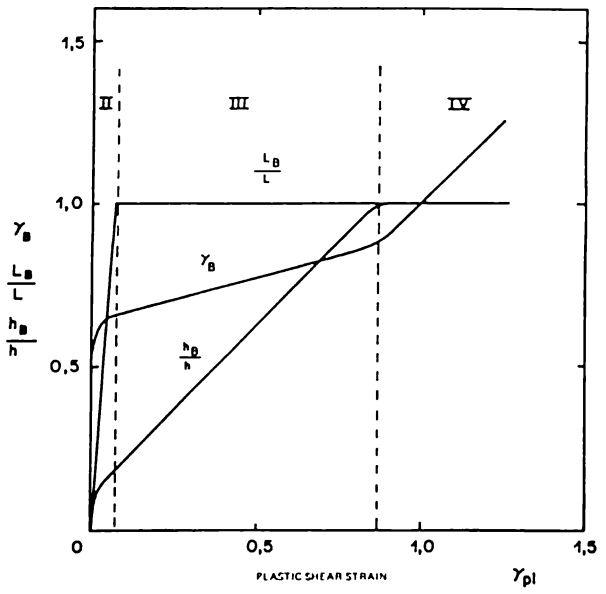

Figure 8. Evolution of shear band parameters during band formation and propagation.

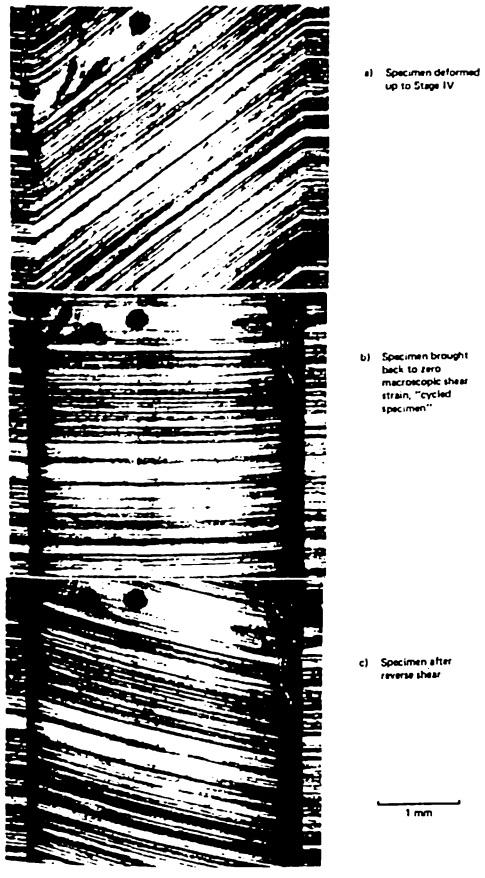

Figure 9. Observation of markers, reverse shear test.

Figure 10. a) Shear band tip at the end of Stage II (PC 133).

Figure 10. b) Shear band tip, Stage III (PC 133).

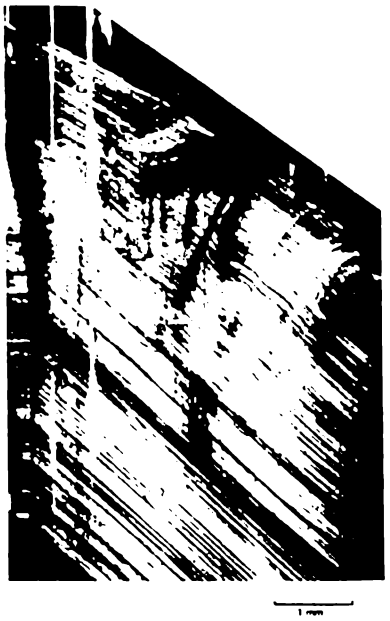

Figure 10. c) Band end in Stage IV.

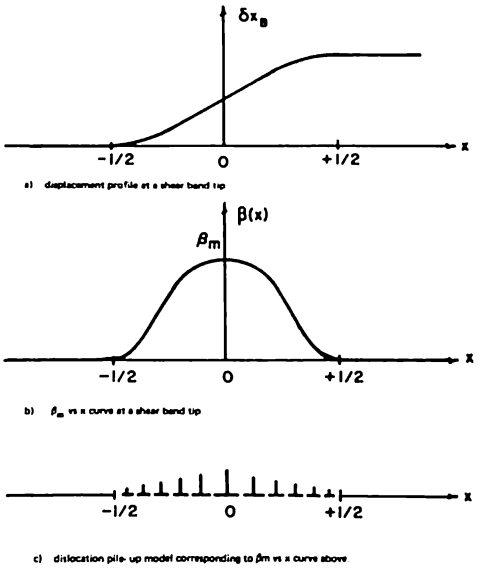

Figure 11.

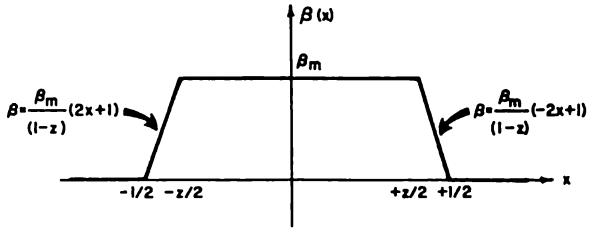

Figure 12. Approximation of β_m used in the calculations.

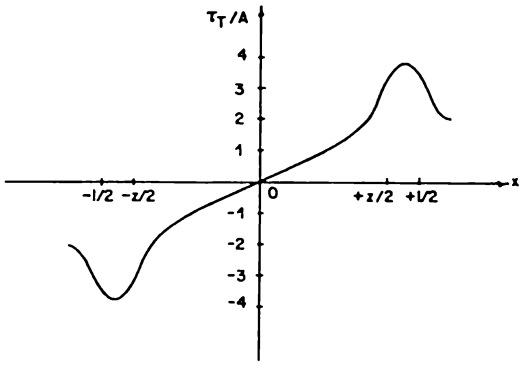

Figure 13. Calculated stress τ_t at a shear band tip.

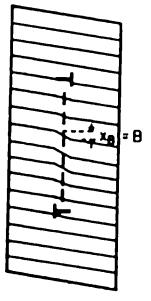

Figure 14. Shear band viewed as an edge dislocation dipole.

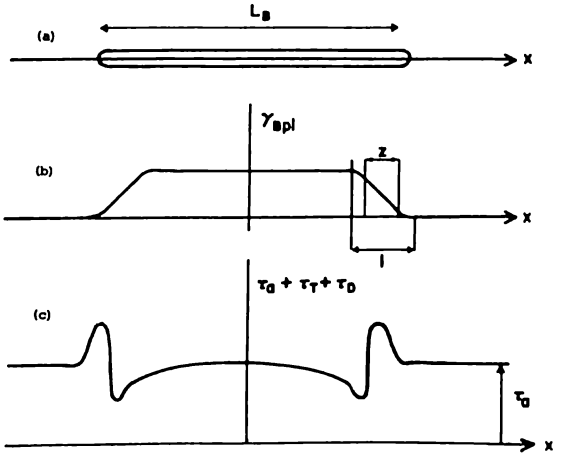

Figure 15. a) Shear band geometry.
b) Shear strain distribution along shear band.
c) Shear stress along band, taking applied stress into consideration.

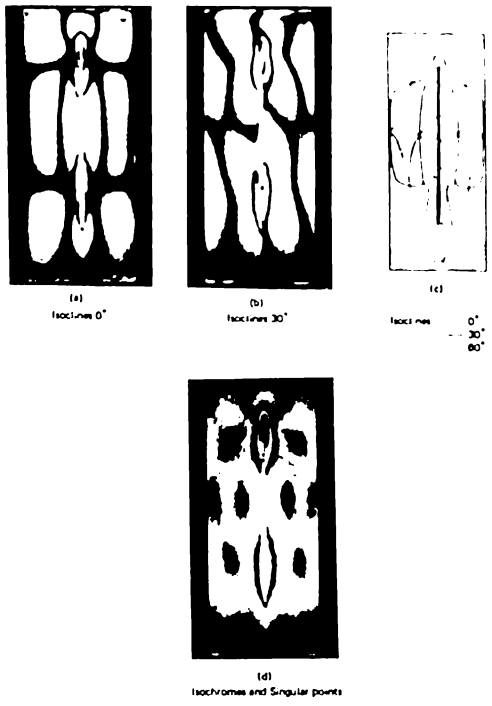

Figure 16. Resumé of photoelasticimetry results (PC 75).

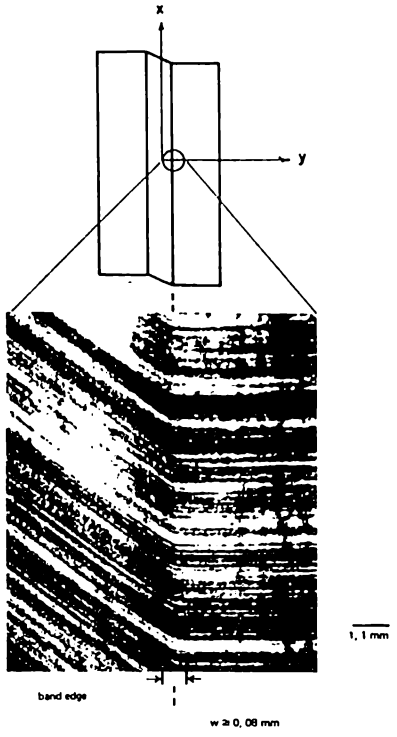

Figure 17. Lateral shear band interface showing the size of w.

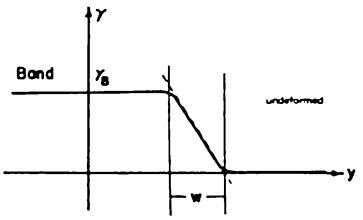

Figure 18. Shear strain distribution at a shear band edge.

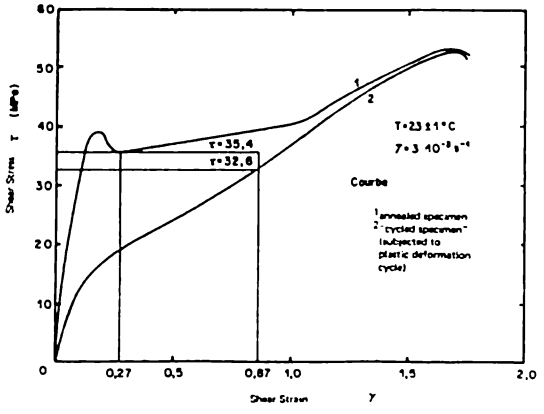

Figure 19. Stress level in Stage III.

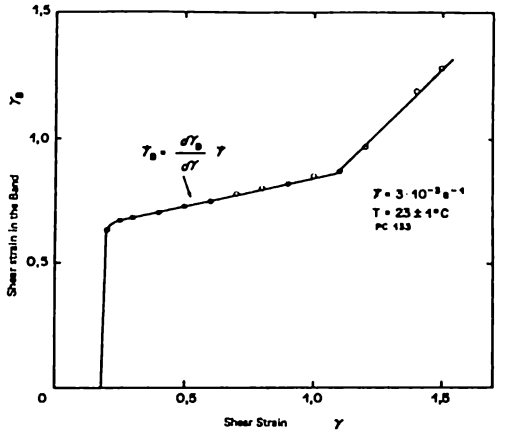

Figure 20. Shear strain in the band γ_B as a function of total shear strain γ.

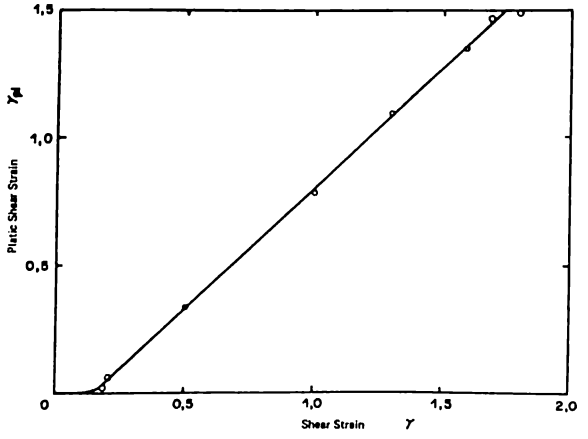

Figure 21. Plastic shear strain γpl vs total shear strain γ.

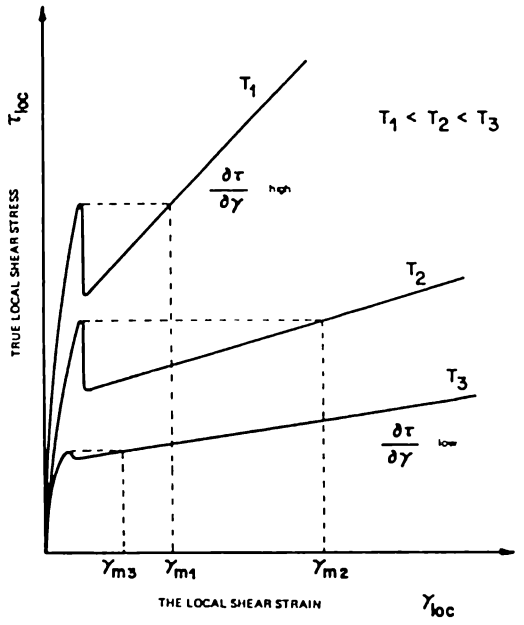

Figure 22. Temperature effects on the intrinsic mechanical response curves.

Appendix: Stress Induced in a Region with Distributed Shear Strain

At a shear band, observation of surface markers on specimens indicate that the local displacement varies from $x_B = B$ (in the band) to zero over a shear band front of length $\ell = 4$mm.

Defining the x axis to be along the band length the displacement x_B will vary along the band as shown by Figure 11a (cf Figure 5). According to Li (1982) such a curve corresponds to a shear strain distribution with a shear strain gradient $\beta = \partial \delta x_B / \partial x$. The function $\beta(x)$ may be defined to represent the slope of the curve $\delta\, x_B\,(x)$. Figure 11b describes this function. By definition we have:

$$\int_{-\infty}^{+\infty} \beta(x)dx \simeq \int_{-\ell/2}^{+\ell/2} \beta(x)dx = B$$

It is proposed to calculate the magnitude of the local shear stress induced by such a shear strain distribution. The local shear strain gradient $\beta(x)$ will be considered to be a pile up of infinitesimal dislocations with Burgers vectors $\beta(x)dx$ and situated at $-\frac{\ell}{2} \leq x \leq +\frac{\ell}{2}$ (Figure 11c). This model was already proposed by Li (1982). The resulting shear stress $\tau(x)$ may now be written:

$$\tau(x) = \int_{x'=-\infty}^{+\infty} \frac{\mu\beta(x')dx'}{2\pi(1-\upsilon)} \frac{1}{(x-x')} = \int_{x'=-\ell/2}^{+\ell/2} \frac{\mu\beta(x')dx'}{2\pi(1-\upsilon)} \frac{1}{(x-x')}$$

A representation of the function $\beta(x')$ which will allow the calculation of $\tau(x)$ must now be found. A simple approach will be to use a step function (Figure A1a). Such a function will, however, have discontinuities at $x = \pm \frac{\ell}{2}$ and the shear stress will be infinitely big at these points [$\tau(-\ell/2) = -\infty$ and $\tau(\ell/2) = +\infty$]. A second possibility will be to use a triangular function (Figure A1b). This will give the maximum value of β, to be $\beta_m = 2B/l$. The shear stress $\tau(x)$ for $0 < x < \ell/2$ will now be written as:

$$\tau(x) = \frac{\mu}{2\pi(1-\upsilon)} \frac{2B}{\ell} \int_{-\ell/2}^{0} \frac{(1+2x'/\ell)}{x-x'} dx' + \frac{\mu}{2\pi(1-\upsilon)} \frac{2B}{\ell} \int_{0}^{\ell/2} \frac{(1-2x'/\ell)}{x-x'} dx'$$

Choosing $A = \frac{\mu}{2\pi(1-\upsilon)} \frac{2B}{\ell}$ and making a variable change such that $(x - x') = u$ gives us:

$$\tau(x) = -A \left[\int_{x+\ell/2}^{x} \frac{1+(2/\ell)(x-u)}{u} du + \int_{x}^{x-\ell/2} \frac{1-(2/\ell)(x-u)}{u} du \right]$$

The magnitude of $\tau(x)$ at different points may now be calculated.

a) at $x = \ell/2$, the equation reduces to

$$\tau(x) = -A \left[\int_{\ell}^{\ell/2} \frac{2-(2/\ell)u}{u} du + \int_{\ell/2}^{0} \frac{2u/\ell}{u} du \right]$$

which gives $\tau(x) = 1.39A$.

b) at $x = 0$, by symmetry, $\tau(0) = 0$

c) away from the shear strain gradient ($x \gg \ell/2$), the effects of the pile up may be viewed as those due to single macroscopic edge dislocation with a Burgers vector $b = \beta_m \ell/2$ located at $x' = 0$, we therefore have:

$$\tau(x) \simeq \frac{\mu}{2\pi(1-\upsilon)} \frac{\beta_m \ell}{2} \left(\frac{1}{x}\right) = A \frac{\ell}{2x}$$

d) inside the gradient ($0 < x < \ell/2$)

$$\frac{\tau(x)}{A} = \int_{x}^{x+\ell/2} \frac{du}{u} + \int_{x}^{x+\ell/2} \frac{2x}{\ell}\,\frac{du}{u} - \int_{x}^{x+\ell/2} \frac{2}{\ell}\,du +$$

$$\int_{x-\ell/2}^{x} \frac{du}{u} - \int_{x-\ell/2}^{x} \frac{2x}{\ell}\,\frac{du}{u} + \int_{x-\ell/2}^{x} \frac{2}{\ell}\,du$$

For the integrals containing $\int du/u$, $u = 0$ represents a singularity but this actually cancel out because

$$\int_{x-\ell/2}^{x} \frac{du}{u} = \int_{\ell/2}^{x} \frac{du}{u}$$

and the resulting equation is:

$$\frac{\tau}{A} = \left(\frac{2x}{\ell} + 1\right) \log\left(\frac{\ell}{2x} + 1\right) - \left(1 - \frac{2x}{\ell}\right) \log\left(\frac{\ell}{2x} - 1\right) \quad 0 \leq x \leq \frac{\ell}{2}$$

The following table gives the values of τ/A at different values of $2x/\ell$.

$2x/\ell$	0	0.01	0.1	0.2	0.4	0.6	0.8	0.9	0.95	1.0
τ/A	0	0.1	0.66	1.04	1.51	1.73	1.74	1.64	1.55	1.39

The shear stress τ attains a maximum value inside the pile up. This is approximately:

$$\tau_{max} \simeq 1.75\,\frac{\mu B}{2\pi(1-\upsilon)}\,\frac{2}{\ell}$$

for $B = 0.075$ mm
$\ell = 4$ mm
$\upsilon = 0.4$

$$\tau_{max} = 14.2 \text{ MPa}$$

This maximum value is not very high due to the rather conservative choice of the triangular $\beta(x)$ function. These calculations can be improved by taking the form of $\beta(x)$ as that shown in Figure A.1c. This function seems to conform better to the shape of the real function as given by Figure 12. The expression for $\tau(x)$ is now given by:

$$\tau(x) = \frac{\mu\beta_m}{2\pi(1-\upsilon)}\left[\frac{1}{(\ell-z)}\int_{-\ell/2}^{-z/2}\frac{(2x'+\ell)}{x-x'}\,dx' + \int_{-z/2}^{+z/2}\frac{dx'}{x-x'} + \frac{1}{(\ell-z)}\int_{z/2}^{\ell/2}\frac{(-2x'+\ell)}{x-x'}\,dx'\right]$$

Choosing $A = \dfrac{\mu\beta_m}{2\pi(1-\upsilon)}$ and $u = x-x'$

$$\frac{\tau(x)}{A} = \frac{1}{\ell-z}\int_{x+z/2}^{x+\ell/2}\frac{\ell+2x-2u}{u}\,du + \int_{x-z/2}^{x+z/2}\frac{du}{u} + \frac{1}{\ell-z}\int_{x-\ell/2}^{x-z/2}\frac{\ell+2x+2u}{u}\,du$$

Since the $\tau(x)$ function is symmetrical with respect to the origin, integration may be done only in the interval $0 \leqslant x \leqslant \ell/2$. Taking the discontinuity of the $1/u$ function at $u = 0$ into consideration, the integration will be split into two expressions valid in the intervals $z/2 < x \leqslant \ell/2$ and $0 \leqslant x \leqslant z/2$.

a) in the interval $z/2 < x \leqslant \ell/2$

$$\frac{\tau}{A} = \frac{\ell+2x}{\ell-z}\int_{x+z/2}^{x+\ell/2}\frac{du}{u} + \int_{x-z/2}^{x+z/2}\frac{du}{u} - \frac{\ell-2x}{\ell-z}\int_{\varepsilon}^{\ell/2-x}\frac{du}{u} + \frac{\ell-2x}{\ell-z}\int_{\varepsilon}^{x-z/2}\frac{du}{u}$$

The last two terms take into account that $u = 0$ at $x = \ell/2$, in a similar manner as for the previous calculations it can be shown that:

$$\int_{x-\ell/2}^{x-z/2}\frac{du}{u} = \int_{\ell/2-x}^{x-z/2}\frac{du}{u}$$

Choosing $z/\ell = \alpha$, the expression becomes:

$$\frac{\tau}{A} = \frac{1}{(1-\alpha)}\left[\left(1+\frac{2x}{\ell}\right)\ln\left(1+\frac{\ell}{2x}\right) - \left(\alpha+\frac{2x}{\ell}\right)\ln\left(1+\frac{\alpha\ell}{2x}\right) + \left(\alpha-\frac{2x}{\ell}\right)\ln\left(1-\frac{\alpha\ell}{2x}\right) - \left(1-\frac{2x}{\ell}\right)\ln\left(\frac{\ell}{2x}-1\right)\right] \quad \text{for} \frac{z}{2} < x \leqslant \frac{\ell}{2}$$

The following table gives some values of τ/A for $\alpha = 0.8$.

$2x/\ell$	0.82	0.85	0.90	0.95	0.98
τ/A	3.48	3.73	3.89	3.79	3.56

b) in the interval $0 \leq x \leq \frac{z}{2}$

$$\frac{\tau}{A} = \frac{\ell + 2x}{\ell - z}\left[\int_{x+z/2}^{x+\ell/2} \frac{du}{u} - \int_{\varepsilon}^{z/2-x} \frac{du}{u} + \int_{\varepsilon}^{x+z/2} \frac{du}{u} - \frac{\ell-2x}{\ell-z}\int_{\varepsilon}^{\ell/2-x} \frac{du}{u}\right]$$

In this case $u = 0$ at $x = z/2$. Using $\alpha = z/\ell$, the final expression becomes:

$$\frac{\tau}{A} = \frac{1}{(1-\alpha)}\left[\left(1 + \frac{2x}{\ell}\right)\ln\left(1 + \frac{\ell}{2x}\right) - \left(\alpha + \frac{2x}{\ell}\right)\ln\left(1 + \frac{\alpha\ell}{2x}\right) + \left(\alpha - \frac{2x}{\ell}\right)\ln\left(\frac{\alpha\ell}{2x} - 1\right) - \left(1 - \frac{2x}{\ell}\right)\ln\left(\frac{\ell}{2x} - 1\right)\right]$$

$$\text{for } 0 \leq x \leq \frac{z}{2}$$

Using the same value for α (= 0.8) the following table completes the preceding one. The curve showing τ/A as a function of X is shown in Figure 13.

$2x/\ell$	0.20	0.50	0.70	0.79
τ/A	0.45	1.26	2.12	3.22

The value of $\tau(x)$ attains a maximum value given by the expression

$$\tau_{max} = 3.89 \frac{\mu}{2\pi(1-\upsilon)} \frac{2B}{\ell(1+\alpha)}$$

For B = 0.075mm
ℓ = 4mm
υ = 0.4
μ = 820 MPa
α = 0.8

τ_{max} = 45.2 MPa